Angular Distribution Studies for the Time-Reversed Photoionization Process in Hydrogenlike Uranium: The Identification of Spin-Flip Transitions

Th. Stöhlker[1,2], T. Ludziejewski[2,3], F. Bosch[2], R.W. Dunford[4], C. Kozhuharov[2], P.H. Mokler[2], H.F. Beyer[2], O. Brinzanescu[2,5], F. Franzke[2], J. Eichler[6], A. Griegal[7], S. Hagmann[8], A. Ichihara[9], A. Krämer[1,2], D. Liesen[2], H. Reich[2], P. Rymuza[3], Z. Stachura[10], M. Steck[2], P. Swiat[11], and A. Warczak[11]

[1]*Institut für Kernphysik, University of Frankfurt, 60486 Frankfurt, Germany*

[2]*Gesellschaft für Schwerionenforschung, 64220 Darmstadt, Germany*

[3]*Institute for Nuclear Studies, 05-400 Świerk, Poland*

[4]*Chemistry Divison, Argonne Nat. Lab., Argonne, Il 60439 USA*

[5]*National Institute for Laser, Plasma and Radiation Physics, 76900 Bucharest-Magurele, Romania*

[6]*Bereich Theoretische Physik, Hahn-Meitner-Institut Berlin, 14109 Berlin, Germany and Fachbereich Physik, Freie Universität Berlin, 14195 Berlin, Germany*

[7]*College of New Jersey, Dept. of Physics, New Jersey, USA*

[8]*Kansas State University, Kansas, USA*

[9]*Japan Atomic Energy Research Institute, Tokai-mura, Ibaraki 319-11, Japan*

[10]*Institute of Nuclear Physics, 31-342 Cracow, Poland*

[11]*Institute of Physics, Jagiellonian University, 30-059 Cracow, Poland*

Abstract

The K-shell photoelectric effect for a hydrogenlike U^{91+} ion is studied by its time-reversed process occurring in relativistic collisions between bare uranium ions and low-Z target atoms. In the time-reversed situation, an electron is captured into the 1s-ground state with the simultaneous emission of a photon.

We present an angular differential study of these transitions for laboratory observation angles between nearly 0° and 150°. Our observation of photon emission close to 0° allowed us to identify spin-flip contributions to the photoionization process and to determine their relative strength.

Photoionization is one of the most important interaction processes between radiation and matter [1,2]. We have previously shown that for high-Z ions photoionization is studied best via its inverse reaction, radiative electron capture (REC) [3–5] in energetic ion-atom collisions [6]. For very high-Z systems, relativistic effects become important and require an exact theoretical treatment [1,7,8] adopting relativistic electron wave functions and including retardation, i.e. all multipole orders of the photon field [9]. For the quantitative assessment of relativistic effects in high-Z ions, angular distributions are a very sensitive probe [10]. This has already been shown for direct photoionization of neutral atoms at high energies ($>$ 500 keV), where retardation leads to a strong forward peaking of the photoelectron angular distribution and where spin-flip effects were observed close to 0° (see e.g. [11]). The inverse reaction for a pure hydrogenlike system lends itself to a different critical test, namely measuring the deviation from a $\sin^2\theta$ distribution. For REC into the K shell of bare nonrelativistic ions, this reference distribution comes about by the cancellation between the effects of retardation on the one hand and the Lorentz transformation into the laboratory system on the other hand [13,14]. Similar cancellations for various atomic processes are known to occur also in relativistic systems [15]. For high enough charges and energies, however, these cancellations are no longer complete. In particular for $Z = 92$ and for REC into the K shell, a significant cross section at forward angles has been predicted and shown to be a unique signature of spin-flip transitions [4,8,16].

In this Letter, we report the first experimental study of a complete photon angular distribution for radiative electron capture into the K shell of a bare high-Z ion (uranium, Z=92). Our measurements encompass laboratory observation angles from near 0° to 150°, permitting the identification of spin-flip contributions that lead to photon emission at 0°. Photon emission at 0° and at 180° is forbidden by angular momentum conservation unless a magnetic spin-flip transition accounts for the spin of the emitted photon [16]. Furthermore, we deduce the electron angular distribution following photoionization of hydrogenlike uranium, i.e. for an explicitly point Coulombic high-Z system. This is at present not accessible in the direct channel due to the lack of the necessary luminosity.

This experiment became possible with the availability of high brilliance heavy ion beams at the ESR storage ring at GSI-Darmstadt [17]. Typically, 10^8 bare $^{238}U^{92+}$ ions were accumulated in the ring at the energy of 309.7 MeV/u and cooled by electrons. A highly useful effect of electron cooling is that the ion energy is locked to a value determined by the acceleration voltage of the cooler. This also reduces the relative momentum spread to about $5{\cdot}10^{-5}$ and provides a small beam size with a diameter close to 2 mm. After ion accumulation, the internal gas-jet was switched on producing a N_2 target of approximately 10^{12} particles/cm^2 areal density. The beam/gas-jet interaction zone was determined to have a diameter of 5 mm. The jet target was equipped with a specially designed scattering chamber which now allows us to measure simultaneously the photon emission at $\approx 0°$, 35°, 60°, 90°, 120°, and 150° with respect to the beam axis. In all cases, planar Ge(i) detectors were used (crystal thicknesses between 12 mm and 15 mm), separated from the ultra-high vacuum of the ESR beam line by either 50 μm stainless steel or 100μm beryllium windows. Except for 0°, all detectors were equipped with x-ray collimator slits, defining the effective active area of the detectors (depending on the observation angle in the range between 200 mm^2 and 800 mm^2 at a typical distance to the jet-target of 350 mm). The chosen collimator dimensions made it possible to resolve the splitting of the Ly-α transitions into the Ly-α_1 and Ly-α_2 components (4.5 keV in the emitter frame). Projectiles having captured one electron were registered downstream beyond the next dipole magnet in a fast scintillator detector with a detection efficiency close to 100%. Only projectile x-rays which were in coincidence with these down-charged U^{91+} ions were recorded. In Fig. 1 an x-ray spectrum measured at 150° in coincidence with electron capture is displayed (laboratory frame). Here, the most prominent feature is due to radiative capture into the K shell of the projectile where the line width results from the momentum distribution of the quasi-free electrons bound in the N_2 molecule. Electron capture into excited states (L, M, and higher shells) leads via cascades to the characteristic Lyman ground-state transitions with a narrow line profile.

For observation of x-rays in the forward hemisphere near the beam at 4.6°, the experiment benefits considerably from the clean experimental environment at the storage ring. In conventional single pass experiments with relativistic beams and solid targets, the production of secondary electrons and its related bremsstrahlung prevents photon detection close to the beam. In the current experiment, x-ray detection at almost 0° was accomplished by using a germanium detector with four independent segments, each furnished with an individual readout. The horizontal and vertical size of each segment is 13 and 25 mm, respectively. The detector was mounted on a movable support, 510 mm down-stream from the projectile-target interaction region. Periodically, after the accumulation procedure was finished, the detector was positioned at a perpendicular distance of just 1 cm from the circulating beam. For the first stripe, this position corresponds to a mean observation angle of 4.6° with an angular acceptance of $\Delta\theta = \pm 0.7°$. In Fig. 2, a coincident x-ray spectrum, measured with the innermost segment of the Ge(i)-detector is displayed. The K-REC line can be well identified at an x-ray energy of 660 keV. In addition, the Lyman transitions measured with the germanium detector are shown separately in the inset, demonstrating the good energy resolution obtained.

The procedure for data reduction has been described in detail elsewhere [18]. All x-ray spectra were first energy calibrated and corrected for detection efficiency. Thereafter, the K-REC line-profiles were fitted using a theoretical line shape based on the double differential cross section [8] which incorporates the correct Compton profiles of the target electrons. This method was applied to all spectra observed at the different observation angles, except for the one of the four fold detector close to 0°. Here, the yield of K-REC photons was obtained from the sum of all events belonging to the relevant energy regime, subtracting a linear background. Since the determinations of absolute cross section values typically result in 30% precision, we concentrate in the following on the relative differential cross sections which are much more precise. For this purpose we exploit the simultaneously observed Ly-α_2+**M1** transitions. Since the Ly-α_2 and the **M1** transitions arise from the decay of the $2p_{1/2}$ and the $2s_{1/2}$ levels, the corresponding line intensity is isotropic in the emitter frame and, consequently, its intensity pattern as function of the laboratory observation angle is exactly known (see e.g. [14]). It is simply given by the relativistic solid angle transformation which allows for an *in situ* relative normalization of all x-ray spectra by taking the Ly-α_2+**M1** as a reference line. The advantage of this technique is that the uncertainty caused by the determination of the solid angle cancels out completely. For determination of the K-REC angular distribution, the only remaining uncertainty is introduced by the efficiency calibration. The latter was determined by using an absolutely calibrated mixed γ-source (see e.g. Ref. [18]). We conservatively assume that the efficiency correction introduces an uncertainty of less than 5%.

In Fig. 3, the measured differential cross sections for REC into the K shell of U^{92+} are presented as a function of the laboratory observation angle (solid triangles) and compared with predictions based on rigorous relativistic calculations [8,16]. These calculations use exact Coulomb-Dirac bound-state and continuum wave functions and take into account the finite nuclear size and all multipole orders up to about $L = 20$. In order to achieve convergence, the summation was carried out over all electron partial waves with Dirac quantum numbers $|\kappa| \leq 20$. To facilitate a comparison of experimental and theoretical cross sections, the measured angular distribution was normalized to the theoretical prediction at 90°. As seen in the figure, good agreement is obtained between the experimental data and the rigorous relativistic calculations. In order to elucidate the necessity of a complete relativistic treatment for high-Z projectiles, the figure also includes the $\sin^2\theta$ distribution following from a nonrelativistic treatment which incorporates the full retardation as well as the Lorentz transformation to the laboratory frame. Obviously, the experimental data deviate considerably from symmetry around 90°. Most importantly, the large cross section observed close to 0° is at variance with the assumption of a spinless electron or a passive electron spin. Rather, in a complete relativistic treatment, the interaction of the electron magnetic moment with the magnetic field produced by the fast moving projectile gives rise to spin-flip transitions which compensate the angular momentum carried away by the photon. Therefore, our measurement close to 0° provides an unambiguous identification of spin-flip transitions occurring in relativistic ion-atom collisions. This effect, predicted recently [4,8,16], has not been confirmed experimentally up to now. For example, for the case of Xe^{54+} $\rightarrow$Be collisions at 197 MeV/u [19], no relativistic effects were observed and the measured K-REC angular distribution could be well reproduced by the nonrelativistic theory. It should also be mentioned that in the relativistic Sauter approximation [20], in which the matrix element of the photoelectric effect is treated in the lowest order of αZ (α is the fine-structure constant) spin-flip contributions at forward angles do not occur. Hence, the present results indicate that higher orders in αZ (automatically contained in the exact wave functions) are needed.

In order to elucidate the physics of the REC process and its relation to photoionization in more detail, we normalize the measured K-REC x-ray yield directly to the intensity of the simultaneously observed Ly-α_2+**M1** line. By applying this technique of normalization, we obtain the REC angular distribution in the emitter frame. This requires only the Lorentz transformation (see e.g. Ref. [16]) of the observation angle. In Fig. 4, the result for this ratio is depicted as a function of the emission angle in the emitter frame (cf. the x-axis at the bottom) along with the corresponding prediction by the rigorous relativistic theory. As can be observed in the figure, both the experimental and the theoretical angular distributions exhibit a pronounced backward shift, since the strong retardation effect (equivalently, the contribution of high multipole orders) is no longer canceled by the Lorentz transformation to the observer system. The maximum of the distribution is now localized close to 150° and the cross section decreases drastically by more than a factor of 40 when going to 0°. Here, indeed the occurrence of spin-flip transitions (compare shaded area in Fig. 4) appears to be a tiny effect with an almost isotropic distribution. This is in obvious contrast to the distribution in the laboratory frame, where the Lorentz transformation not only compensates retardation but also amplifies the relative weight of the spin-flip transitions close to 0° by more than an order of magnitude with respect to the maximum of the distribution.

From the experimental REC distribution in the emitter frame, the corresponding angular distribution for photoionization can also be derived by simply replacing the REC angle θ' with $\pi - \theta'$ since the directions of the photon and the electron are interchanged. Therefore, the upper abscissa in Fig. 4 refers to the electron angular distribution for photoionization of hydrogenlike uranium at the corresponding photon energy of 272 keV. We note, that contrary to conventional photoionization studies for high-Z elements where scattering inside the solid targets leads to a considerable broadening of the photoelectron emission angle [12], no such effects have to be considered here. Moreover, compared to direct photoionizaton experiments the observed spin-flip transitions are found at a lower energy because in our experiment this effect appears to be enhanced by the Lorentz transformation. While, on the theoretical side, neither screening effects nor electron correlations are of importance for the K-shell photoeffect in neutral atoms at high energies [1], we here have the advantage of a very "clean" single-electron case with the potential for precision studies of photoionization via the inverse reaction.

In summary, we measured the photon angular distribution for radiative electron capture into the K shell of U^{92+} from N_2 at a collision energy of 309.7 MeV/u corresponding to the time-reversed process of photoionization of hydrogenlike uranium at a photon energy of 272 keV. By measuring at observation angles from nearly $0°$ to $150°$, distinctive relativistic corrections were detected which bend the angular distribution into the forward hemisphere. In particular, the observation of photon emission close to $0°$ allowed us to identify spin-flip contributions to the differential K-REC cross sections for the first time. In this way, for a high projectile charge and relativistic projectile motion, the electron spin manifests itself in a particularly clear-cut manner as was theoretically predicted recently. At the same time, the experiment allowed us to measure the otherwise inaccessible electron angular distribution for photoionization of hydrogenlike uranium U^{91+}, i.e. for an explicitly point Coulombic high-Z system. This finding emphasizes the importance of the REC process for the study of photoionization in the domain of high-Z one- and few-electron ions.

R.W.D. and S.H. were supported by the U.S. D.O.E. Office of Basic Energy Sciences, Division of Chemical Sciences. The support by the State Committee of Scientific Research (Poland) under research grant No. 2P03B10910 and No. 2P03B11615 and by the german-polish collaboration grant WTZ (POL-229-96) is acknowledged.

REFERENCES

[1] For a summary of the atomic photoeffect, see, e.g., R.H. Pratt, A. Ron, and H.K. Tseng, Rev. Mod. Phys. **45** 273 (1973).

[2] B. Craseman, X-Ray and Inner-Shell Process 1996 (AIP, Woodbury, New York, 1997), p. 3.

[3] P.H. Mokler and Th. Stöhlker, Adv. in Atomic, Molecular, and Optical Physics, Vol.37, 297 (1996).

[4] A. Ichihara, T. Shirai, and J. Eichler, Phys. Rev. A **54**, 4954 (1996).

[5] Th. Stöhlker et al., Phys. Rev. Lett. **79**, 3270 (1997).

[6] In the present context, we are dealing with capture from very light atoms, here N_2, so that the bound target electrons can be considered as quasi-free. The corrections caused by the momentum distribution in the target atom have been shown to be at the one percent level for the cases considered (see Ref. [4]).

[7] W.R. Alling and W.R. Johnson, Phys. Rev. **139**, A1050 (1965).

[8] A. Ichihara, T. Shirai, and J. Eichler, Phys. Rev. A **49**, 1875 (1994).

[9] H.R. Hulme, J. McDougall, R.A. Buckingham, and R.H. Fowler, Proc. Roy. Soc. (London) **A149**, 131 (1935).

[10] A.F. Starace, in *Corpuscles and Radiation in Matter I* edited by W. Mehlhorn, Handbuch der Physik **31**, 1 (Springer Verlag, Berlin 1982).

[11] H.K. Tseng et al., Phys. Rev. A **17**, 1061 (1978).

[12] S.J. Blakeway et al., J. Phys. B: At. Mol. Phys. **16** 3752 (1983).

[13] E. Spindler, H.-D. Betz and F. Bell, Phys. Rev. Lett. **42**, 832 (1979).

[14] J. Eichler and W.E. Meyerhof *Relativistic Atomic Collisions* (Academic Press, San

Diego, 1995).

[15] A. Ron et al., Phys. Rev. A **50**, 1312 (1994).

[16] J. Eichler, A. Ichihara, and T. Shirai, Phys. Rev. A **51**, 3027 (1995).

[17] K. Blasche, B. Franzke, *Proc. of the 4th Europ. Part. Acc. Conf.*, V. Suller and Ch. Petit-Jean-Genaz eds., World Scientific, Singapore, 1994, 133–137.

[18] Th. Stöhlker et al., Phys. Rev. A **58** 2043 (1998).

[19] R. Anholt et al., Phys. Rev. Lett. **53** 234 (1984).

[20] F. Sauter, Ann. Physik **9** 217 (1931); **11** 454 (1931).

FIGURES

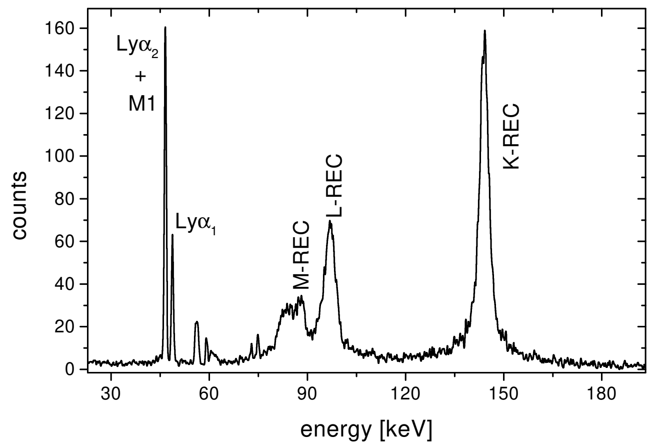

FIG. 1. X-ray spectra obtained at 150° observation angle for U^{92+} collisions at 309.7 MeV/u in coincidence with electron capture.

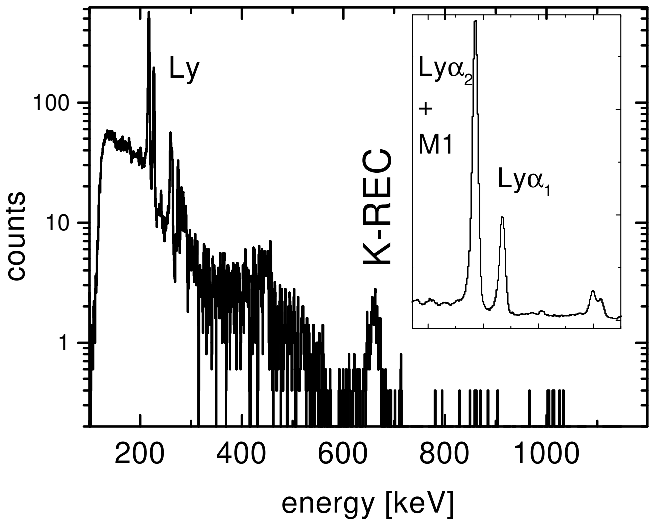

FIG. 2. X-ray spectra obtained at nearly 0° observation angle for U^{92+} collisions at 309.7 MeV/u in coincidence with electron capture. The inset displays the subshell resolved Lyman transitions.

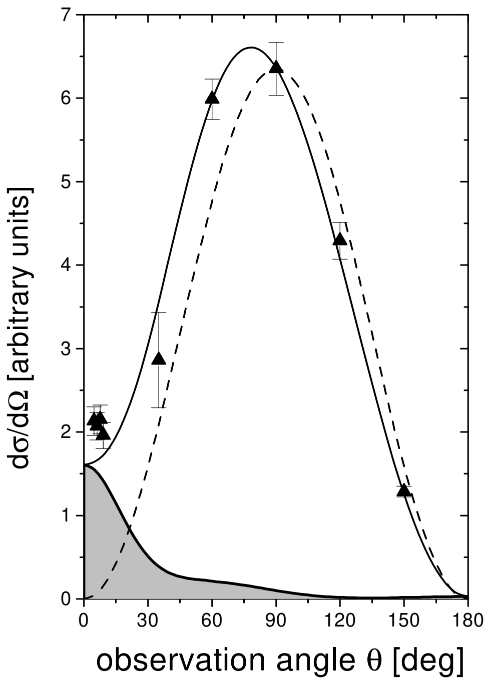

FIG. 3. Angular distribution for REC into the K shell of bare uranium (solid triangles) as a function of the observation angle θ (309.7 MeV/u $U^{92+} \rightarrow N_2$). The solid line refers to complete relativistic calculations and the shaded area to the spin-flip contributions [8,16]. The $\sin^2\theta$ shape of the nonrelativistic theory is given by the dashed line. The absolute values of the experimental data and of the nonrelativistic theory are normalized to the result of the complete calculations at 90°.

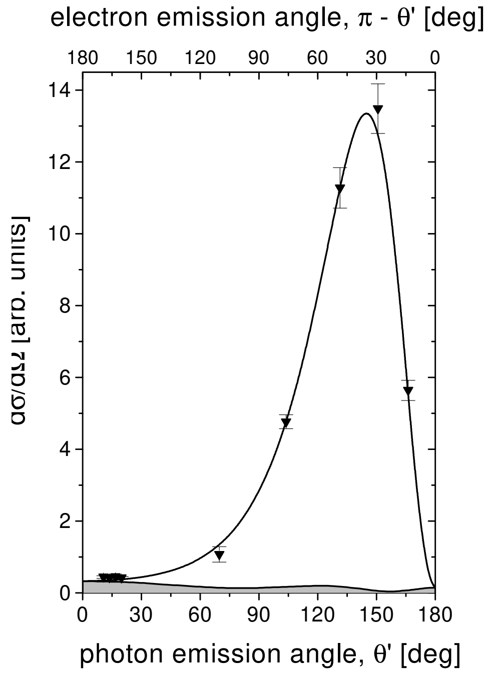

FIG. 4. K-REC angular distribution (projectile frame) as a function of the emission angle θ' (bottom x-axis). The x-axis at the top refers to the corresponding electron angular distribution for photoionization of H-like uranium (photon energy 272 keV) obtained by the interchanging θ' by $\pi - \theta'$. The full line gives the photoionization distribution as obtained from complete relativistic calculation whereas the shaded area depicts the spin-flip contribution.